JCTC Journal of Chemical Theory and Computation

Letter

pubs.acs.org/JCTC

Are DFT Methods Accurate in Mononuclear Ruthenium-Catalyzed Water Oxidation? An ab Initio Assessment

Runhua Kang, Jiannian Yao,* and Hui Chen*

Beijing National Laboratory for Molecular Sciences (BNLMS), CAS Key Laboratory of Photochemistry, Institute of Chemistry, Chinese Academy of Sciences, Beijing, 100190, China

Supporting Information

ABSTRACT: Mononuclear Ru-based water oxidation catalysts (WOCs) are an important class of WOCs for water splitting. In this work, through high-level coupled cluster calculations (CCSD(T)/CBS), we have examined a variety of density functionals for their performances in the whole catalytic cycle of water oxidation catalyzed by mononuclear Ru-based WOCs. The tested functionals cover a wide range from pure GGA and meta-GGA to hybrids and double hybrids (TPSS, OLYP, BP86, M06-L, B3LYP, PBE0, M06, M06-2X, TPSSh, CAM-B3LYP, wB97X, B2-PLYP, B2GP-PLYP). Depending on different reaction types and species in the catalytic cycle, the performances of different DFTs vary severely, whose trends are summarized in the paper. Our results indicate that using a single approximate functional to accurately model all reactions involved in the whole Ru-based WOC catalytic cycle is still a very challenging task. In the current status, PBE0 and M06 may be recommended for the whole catalytic cycle. Generally, this study provides a guide for selecting an appropriate DFT method in modeling each of the various steps in water oxidation catalyzed by Ru-based WOCs. The sensitivity of DFT and ab initio results upon the degree of basis set completeness found in this work is also worthy of attention in the future theoretical study of mononuclear Ru-based WOCs.

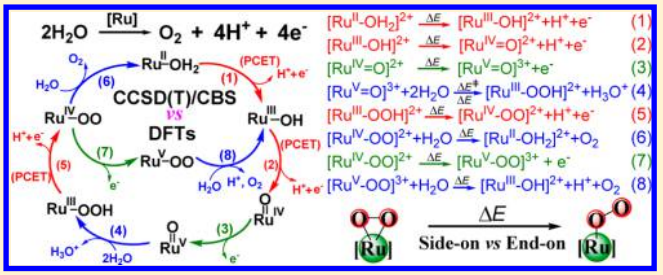

Water oxidation is of crucial importance in sunlight-driven water splitting, which constitutes a promising way to utilize alternative clean and sustainable solar energy in response to an energy crisis and global warming caused by burning fossil fuel.[1] Both in natural photosynthesis and in artificial photosynthesis, water oxidation is a key and difficult reaction for the coupling of proton release, electron transfer, and the formation of an O−O bond ($2H_2O \rightarrow 4H^+ + 4e^- + O_2$). Thus, a catalyst is inevitable in efficient water oxidation. In nature, oxidation of water to generate O_2 is catalyzed by a Mn_4Ca cluster within the oxygen-evolving complex (OEC) of photosystem II with a high efficiency and rate.[2,3] Correspondingly, in artificial photosynthesis, the design and discovery of an effective water oxidation catalyst (WOC) have attracted considerable interest recently.[4−7]

Intense research efforts have been made in the WOC area. Until now, the most extensively studied WOCs are ruthenium-based catalysts. Especially now, it is known that a multinuclear metal center is not a prerequisite for water oxidation, and a single metal site of mononuclear Ru complexes can also catalyze the reaction.[8] The structural simplicity of mononuclear Ru WOCs compared with multinuclear Ru WOCs can greatly facilitate both the catalytic mechanism and structure−activity relationship studies for water oxidation, which have been explored in many experimental and theoretical works.[9−29] Many molecular level details of catalytic processes by Ru-based WOCs have been revealed from theoretical modelings, which are very helpful and insightful in searching for more efficient WOCs.[9−18,21,30−38] Among the theoretical studies, density functional theory (DFT) was employed as a computational modeling tool exclusively, mainly due to the usual large molecular size and high complexity of the Ru WOCs under study. Although DFT methods have achieved great success in transition metal chemistry,[39−45] it is becoming prudent to validate and assess approximate DFT functionals in a specific class of transition metal systems because (1) estimations of errors from approximate functionals can thus be known and (2) given a big variation of computational results often seen between different functionals, finding a well-performing functional for a specific area is surely helpful for the DFT application to be more predictive.[46,47] The concern about DFT performance in ruthenium-catalyzed water oxidation also received attention in the WOC community recently.[30] One straightforward way to address this issue is by comparative study using more accurate ab initio methods. To the best of our knowledge, there is still no assessment reported on DFT performance in any ruthenium-based WOC. It is the goal of this study to provide a first and systematic assessment of popular density functionals in the whole catalytic cycle of mononuclear Ru WOCs. To achieve this goal, we herein employed high level canonical coupled cluster CCSD(T)[48,49] and explicitly correlated coupled cluster CCSD(T)-F12[50] methods (closed-shell and open-shell) as our reference, which was obtained with extrapolation for valence electron correlation to the complete basis set (CBS) limit, and with consideration of Ru 4s4p core−valence correlation.

Received: January 3, 2013
Published: March 20, 2013

   dx.doi.org/10.1021/ct400004j | J. Chem. Theory Comput. 2013, 9, 1872−1879

The mechanism of water oxidation by mononuclear ruthenium-based WOCs has been extensively explored. Concerning the key issue of the O−O formation step, there are several catalytic mechanisms proposed, the most widely accepted one of which is water nucleophilic attack (WNA) to high valent metal oxo (Ru^{V}=O).[51] This mechanism was also known to be the viable one for O−O bond formation with OEC in natural photosynthesis.[52] In addition to the WNA mechanism, there are also other O−O formation mechanisms such as direct coupling via interaction of two metal oxo units (I2M).[14,17,35,51] However, for the O−O formation step in this work we focus on the WNA mechanism due to its wide occurrence in water oxidation as well as in the corresponding theoretical modeling.[10−12,15,17,31,32,36−38,51]

The typical whole catalytic cycle of water oxidation by mononuclear single-site Ru-based WOC taking WNA as an O−O bond formation mechanism is shown in Scheme 1 (unless specified

Scheme 1. Catalytic Cycle for Water Oxidation Catalyzed by the Single-Site Ru Catalyst Following the WNA Mechanism[a]

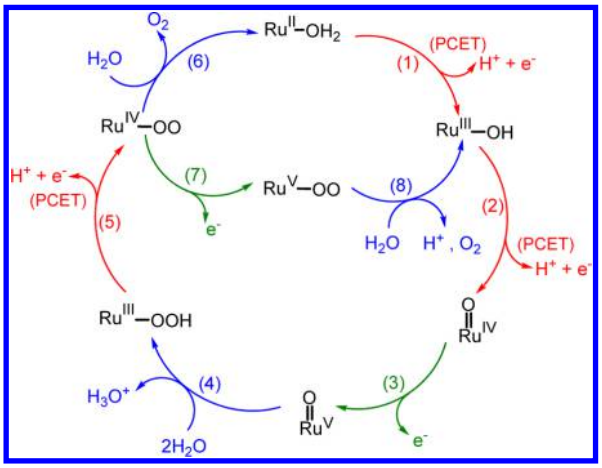

[a]The processes in blue are substitution or addition reactions. The ones in red are PCET O−H bond breaking reactions. The ones in green are pure 1e-oxidation reactions.

otherwise, the supporting ligands of Ru are not shown for clarity throughout this work). Starting from Ru-aqua complex Ru^{II}−OH_2, through two consecutive proton-coupled electron transfers (PCET) by a terminal oxidant (usually is Ce^{IV} in experiment), two O−H bonds are cleaved separately (eq 1 and 2), and a high-valent Ru^{IV}=O species is generated. Further 1e-oxidation (eq 3) can convert Ru^{IV}=O to Ru^{V}=O, which is the active water oxidation species. Subsequent O−O bond formation is accomplished by WNA, concomitantly coupled with proton-transfer (PT) to form hydroperoxo intermediate Ru^{III}−OOH (eq 4). Once formed, the hydroperoxo intermediate undergoes a PCET process to be oxidized to peroxo complex Ru^{IV}−OO (eq 5). Finally, the O_2 is liberated by substitution with a water molecule and at the same time regenerates the initial aqua catalyst Ru^{II}−OH_2 to complete the catalytic cycle (eq 6). Instead of eq 6, it was found that at higher concentrations of acid, Ru^{IV}−OO was further oxidized to Ru^{V}−OO (eq 7), followed by the rapid release of O_2 and deprotonation of substituted water to re-enter the next round of the catalytic cycle (eq 8).[10,29,30] The thermodynamics of all the reactions represented by eqs 1−8 are under study in this work (it should be noted that since eqs 1, 6, 7, and 8 form a thermodynamic cycle, the thermodynamics of one reaction among them is not independent from those of the other three reactions).

According to the Bell−Evans−Polanyi (BEP) principle,[53,54] reaction energy is directly related to the corresponding reaction barrier. For the key WNA O−O bond formation process (eq 4), kinetics is also our concern, for which we calculate the activation energy. By exploring all these aspects of the catalytic cycle, we will be able to give a quite comprehensive assessment of DFT performance for the reaction thermodynamics and kinetics. In addition, the interesting issue of the end-on/side-on (open/closed) Ru−O_2 energy gaps will be addressed at a high computational level in this work. All of this new knowledge about the various energetics would be helpful to future theoretical explorations in the area of Ru-based WOCs.

$$[Ru^{II}-OH_2]^{2+} \rightarrow [Ru^{III}-OH]^{2+} + H^+ + e^- \quad (1)$$

$$[Ru^{III}-OH]^{2+} \rightarrow [Ru^{IV}=O]^{2+} + H^+ + e^- \quad (2)$$

$$[Ru^{IV}=O]^{2+} \rightarrow [Ru^{V}=O]^{3+} + e^- \quad (3)$$

$$[Ru^{V}=O]^{3+} + 2H_2O \rightarrow [Ru^{III}-OOH]^{2+} + H_3O^+ \quad (4)$$

$$[Ru^{III}-OOH]^{2+} \rightarrow [Ru^{IV}-OO]^{2+} + H^+ + e^- \quad (5)$$

$$[Ru^{IV}-OO]^{2+} + H_2O \rightarrow [Ru^{II}-OH_2]^{2+} + O_2 \quad (6)$$

$$[Ru^{IV}-OO]^{2+} \rightarrow [Ru^{V}-OO]^{3+} + e^- \quad (7)$$

$$[Ru^{V}-OO]^{3+} + H_2O \rightarrow [Ru^{III}-OH]^{2+} + H^+ + O_2 \quad (8)$$

In mononuclear Ru WOCs, pyridine- and/or amine-based ligands are widely used. Due to this fact, we used a simplified WOC model shown in Scheme 2 in our highly costly open-shell

Scheme 2. Simplified Models Used in This Work for (a) WNA O−O Formation Reaction (eq 4), and (b) All the Other Reactions (eqs 1−3, 5−8)

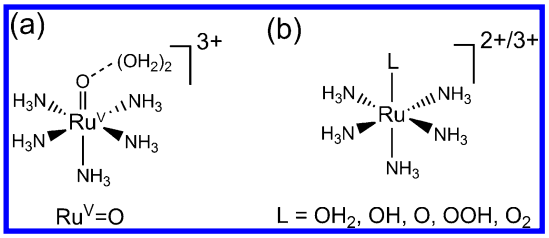

coupled cluster calculations by replacing all N-ligating ligands to NH_3. This WOC model keeps the same charge as most of the commonly used mononuclear Ru WOCs. Despite the simplicity of this model, we consider that it bears the intrinsic characters of larger and more practical Ru WOCs used in experiments. In this work, no solvent effect was considered, and all calculations were performed in the gas phase. This is because this work is mainly for comparison of different electronic structure methods, and we keep the computational chemistry philosophy in mind that electronic structure methods should be reliable first in the gas phase before we can count on them in the more complicated situation of the condensed phase like in solution. To account for the scalar relativistic effect of Ru, relativistic pseudo-potential (PP) ECP28MDF[55] for Ru was used throughout. In our ab initio and DFT calculations, we employed correlation consistent basis sets for all atoms.[55,56] For brevity, we take abbreviations for double-ζ, triple-ζ, and quadruple-ζ correlation consistent basis sets (the corresponding -PP

dx.doi.org/10.1021/ct400004j | J. Chem. Theory Comput. 2013, 9, 1872−1879

Table 1. Calculated Reaction Energies ΔE_R (kcal/mol) for O_2-Release Reaction (eq 6: $[Ru^{IV}{-}OO]^{2+} + H_2O \rightarrow [Ru^{II}{-}OH_2]^{2+} + O_2$) with the CCSD(T) and CCSD(T)-F12b Methods at Various Levels[a]

	CCSD(T)/DZ	CCSD(T)/TZ	CCSD(T)/CBS(DZ-TZ)	CCSD(T)-F12b/ADZ	CCSD(T)-F12b/ATZ	CCSD(T)-F12b/CBS(ADZ-ATZ)
ΔE_R	−21.02	−9.37	−5.28	−6.44	−5.49	−5.11

[a]All data are from valence-only correlation calculations. The $[Ru^{IV}{-}OO]^{2+}$ intermediate calculated here is of singlet spin state and closed structure (side-on O_2 binding), because our calculations show that the side-on structure is much more stable than the end-on one.

Table 2. Calculated Reaction Energies ΔE_R (eqs 1−8), Reaction Barrier $\Delta E^{\ddagger}$ (eq 4), and Side-On/End-On Energy Gaps ΔE_{gap} of RuO_2 Intermediates at the Various CCSD(T) Levels (in kcal/mol)

energetics[a]	ΔE(CCSD(T)/DZ)	ΔE(CCSD(T)/TZ)	ΔE(CCSD(T)/CBS(DZ-TZ))	$\Delta\Delta E_{4s4p}$(CCSD(T)-F12b/DZ)[b]	ΔE_{final}(CBS+4s4p)[c]
$\Delta E_R(1)$	393.05	394.97	395.64	−1.31	394.34
$\Delta E_R(2)$	393.58	399.54	401.63	0.64	402.28
$\Delta E_R(3)$	371.45	372.63	373.05	−1.44	371.61
$\Delta E_R(4)$	−1.08	−0.59	−0.41	−0.09	−0.50
$\Delta E^{\ddagger}(4)$[d]	1.73	3.00	3.44	−0.01	3.43
$\Delta E_R(5)$	403.89	403.35	403.16	−0.71	402.45
$\Delta E_R(6)$	−21.02	−9.37	−5.28	1.67	−3.60
$\Delta E_R(7)$	356.13	361.94	363.99	−0.47	363.52
$\Delta E_R(8)$	15.90	23.65	26.37	0.83	27.21
$\Delta E_{gap}(Ru^{IV}O_2)$[e]	3.61	11.92	14.84	1.19	16.03
$\Delta E_{gap}(Ru^{V}O_2)$[f]	−2.91	4.94	7.70	0.58	8.28

[a]The labels in parentheses after ΔE_R and $\Delta E^{\ddagger}$ denote the corresponding labeling number in Scheme 1 for reactions. [b]Ru 4s4p core−valence correlation corrections to relative energetics ΔE from the CCSD(T)-F12b method with the cc-pwCVDZ-PP basis on Ru and the DZ basis set on the other atoms. [c]Final result combining the valence-only CCSD(T)/CBS value of ΔE and Ru 4s4p core−valence correlation correction $\Delta\Delta E_{4s4p}$. [d]Reaction barrier of reaction 4 in Scheme 1. [e]Energy gap between singlet side-on (closed) structure and triplet end-on (open) structure of $[Ru^{IV}{-}OO]^{2+}$, i.e., isomerization reaction energy of $[Ru^{IV}{-}OO]_{side\text{-}on}{}^{2+} \rightarrow [Ru^{IV}{-}OO]_{end\text{-}on}{}^{2+}$. [f]Energy gap between doublet side-on (closed) structure and quartet end-on (open) structure of $[Ru^{V}{-}OO]^{3+}$, i.e., isomerization reaction energy of $[Ru^{V}{-}OO]_{side\text{-}on}{}^{3+} \rightarrow [Ru^{V}{-}OO]_{end\text{-}on}{}^{3+}$.

suffix for Ru basis set is omitted) as follows, DZ/TZ/QZ for cc-pVDZ/cc-pVTZ/cc-pVQZ and ADZ/ATZ for aug-cc-pVDZ/aug-cc-pVTZ.[55,56] In Ru 4s4p core−valence correlation calculations, correlation consistent weighted core−valence double-ζ basis set cc-pwCVDZ-PP was used.[55] Unless specified otherwise, the most stable spin state and conformation of Ru-containing species in the whole catalytic cycle depicted in Scheme 1 were adopted as follows: S = 0, singlet ($Ru^{II}OH_2$, side-on $Ru^{IV}O_2$); S = 1/2, doublet ($Ru^{III}OH$, $Ru^{III}OOH$, $Ru^{V}O$, side-on $Ru^{V}O_2$); S = 1, triplet ($Ru^{IV}O$). O_2 and H_2O are on their ground spin state, i.e., triplet and singlet, respectively. While not in the shown catalytic cycle, triplet (S = 1) end-on $Ru^{IV}O_2$ and quartet (S = 3/2) end-on $Ru^{V}O_2$ structures are also under study. The small values of T_1 diagnostic[57] results (<0.05, see Table S6 in the Supporting Information) for our CCSD/TZ calculations indicate that our coupled cluster calculations reported herein are reliable. All ab initio calculations were carried out with the MOLPRO program package,[58] and all DFT calculations were done with the Gaussian 09 program package.[59] Other computational details can be found in the Supporting Information (SI) document, and below we focus on our key results.

To have an estimation of the errors for our CCSD(T)/CBS results in terms of basis set incompleteness error (BSIE) with valence electron correlation, we did more expensive and less BSIE-affected explicitly correlated CCSD(T)-F12 calculations for the water-substitutive O_2 release reaction (eq 6) using the ADZ and ATZ basis set, and based on it the CCSD(T)-F12/CBS value was obtained as our most accurate reference here. The results shown in Table 1 indicate that (1) CBS extrapolation for the CCSD(T) calculation based on the DZ−TZ pair of basis sets is absolutely necessary to reduce the otherwise huge BSIE potentially in the current Ru WOC system and (2) the difference between CCSD(T)/CBS (−5.28 kcal/mol) and reference CCSD(T)-F12/CBS (−5.11 kcal/mol) is only 0.17 kcal/mol, indicating that the CCSD(T)/CBS calculation protocol that we adopted here should be adequately reliable in addressing the potential BSIE issue in our coupled cluster calculations.

Using our CCSD(T)/CBS protocol based on DZ and TZ basis sets for valence-only correlation, with the additional consideration of the Ru 4s4p core−valence correlation effect, the calculated reaction energetics data for the whole catalytic cycle were collected in Table 2. In addition, the energy gap between side-on (closed) and end-on (open) Ru−O_2 structures shown in Figure 1, whose values had never been determined by a high level ab initio method, is an interesting issue to be clarified. Thus, as shown in Table 2, we also explored the side-on/end-on energy gaps for $[Ru^{IV}{-}OO]^{2+}$ and $[Ru^{V}{-}OO]^{3+}$ intermediates.

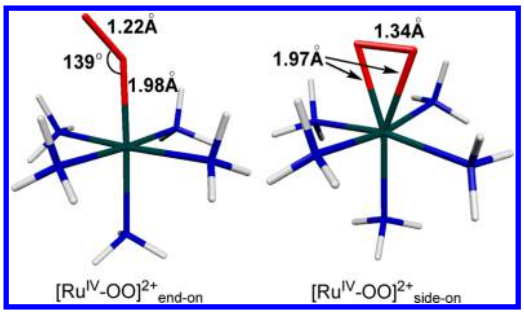

Figure 1. Optimized geometries of end-on (triplet) and side-on (singlet) $[Ru^{IV}{-}OO]^{2+}$.

From those data in Table 2, some features are noteworthy. (1) First, for some reactions like 2, 6, 7, and 8, and end-on/side-on gaps of $[Ru^{IV}{-}OO]^{2+}$ and $[Ru^{V}{-}OO]^{3+}$ intermediates, CCSD(T) calculations with smaller DZ basis set show very large BSIEs, which can be seen from the significant improvements when using a larger TZ basis set. Among reactions 2, 6, 7, and 8,

dx.doi.org/10.1021/ct400004j | J. Chem. Theory Comput. 2013, 9, 1872−1879

Table 3. Deviations of All DFT/QZ Computational Energetics (kcal/mol) from the Reference Coupled Cluster Reference Data (CBS+4s4p) in Table 2[a]

energetics[b]	B3LYP	PBE0	BMK	BP86	CAM-B3LYP	M06	M06-2X	M06-L	TPSS	TPSSh	wB97X	B2GP-PLYP	B2-PLYP	OLYP
$\Delta E_R(1)$	−3.76	−5.99	−8.23	−10.62	−3.50	−4.48	3.26	−8.94	−11.94	−8.94	−0.64	−2.81	−5.08	−11.47
$\Delta E_R(2)$	−1.44	−2.44	11.21	−7.72	0.89	−1.77	3.99	−7.92	−8.23	−5.12	2.12	−8.53	−10.03	−13.29
$\Delta E_R(3)$	7.07	6.10	7.51	−0.97	9.84	4.50	13.07	−0.81	−1.09	2.51	7.78	−1.16	−1.37	−4.52
$\Delta E_R(4)$[c]	2.19 (4.12)	−1.76 (0.75)	−17.81 (−14.26)	14.61	−6.34 (−2.68)	0.77 (2.14)	−15.25 (−11.85)	12.18	11.58	5.16 (6.67)	−8.84 (−5.07)	−1.58	3.36	15.51
$\Delta E^{\ddagger}(4)$[c,d]	0.69 (1.97)	−0.34 (1.00)	−3.90 (−0.74)	2.13	−1.20 (0.78)	1.90 (2.44)	−3.76 (−1.36)	4.20	1.42	0.38 (1.45)	−0.52 (1.23)	7.95	4.34	3.80
$\Delta E_R(5)$	9.72	5.96	13.05	3.99	9.12	6.28	8.43	3.43	1.29	3.34	9.11	−2.60	−1.27	1.87
$\Delta E_R(6)$	−8.72	−8.43	−12.60	6.28	−12.42	−4.84	−18.99	−1.09	5.55	−0.45	−16.18	−1.70	−0.85	−2.15
$\Delta E_R(7)$	−3.54	−5.91	−0.72	−10.21	−1.08	−5.27	3.06	−13.69	−10.33	−7.55	−3.75	9.91	4.02	−17.41
$\Delta E_R(8)$	−8.94	−8.51	−20.11	5.86	−14.85	−4.05	−18.79	3.66	3.94	−1.84	−13.06	−14.42	−9.96	3.79
$\Delta E_{gap}(Ru^{IV}O_2)$[e]	−16.88	−14.96	−12.73	−13.32	−14.99	−13.19	−15.30	−15.37	−11.48	−12.28	−15.56	−3.89	−6.30	−19.07
$\Delta E_{gap}(Ru^{V}O_2)$[f]	−9.02	−8.48	−19.39	6.87	−12.74	−3.73	−19.84	−1.12	5.26	−0.98	−14.58	−11.71	−7.11	0.96

[a]The deviation values in this table are computed from ΔE(DFT) − ΔE(CCSD(T)); thus a negative value means a smaller DFT value than the CCSD(T) reference value. [b]The labels in parentheses after reaction energy ΔE_R and reaction barrier $\Delta E^{\ddagger}$ denote the corresponding labeling number in Scheme 1 for reactions. [c]The results after spin-projected corrections for those cases with apparent spin-contamination are inside parentheses. [d]Reaction barrier of the reaction 4 in Scheme 1. [e]Energy gap between the singlet closed structure and triplet open structure of $[Ru^{IV}{-}OO]^{2+}$, i.e., isomerization reaction energy of $[Ru^{IV}{-}OO]_{side\text{-}on}^{2+} \rightarrow [Ru^{IV}{-}OO]_{end\text{-}on}^{2+}$. [f]Energy gap between doublet closed structure and quartet open structure of $[Ru^{V}{-}OO]^{3+}$, i.e., isomerization reaction energy of $[Ru^{V}{-}OO]_{side\text{-}on}^{3+} \rightarrow [Ru^{V}{-}OO]_{end\text{-}on}^{3+}$.

reaction 6 of O_2 release from $[Ru^{IV}{-}OO]^{2+}$, which is used to assess our CBS protocol above as shown in Table 1, exhibits the largest BSIE by having a difference of about 16 kcal/mol between DZ and CBS values. For end-on/side-on gaps of $Ru{-}O_2$ intermediates, BSIE with the DZ basis set is also significant for both $[Ru^{IV}{-}OO]^{2+}$ and $[Ru^{V}{-}OO]^{3+}$. Thus, compared with DZ values, the CBS values increase the stability of side-on structures to end-on ones by more than 10 kcal/mol. The TZ basis set even changes the sign of the DZ gap result from negative (−2.91 kcal/mol) to positive (4.94 kcal/mol) for $[Ru^{V}{-}OO]^{3+}$. Considering the fact that all the systems under study are of high cationic character, such huge BSIEs are very surprising and were never observed in our previous coupled cluster calculations for other 3d, 4d, and 5d transition metal systems.[60−65] This sensitivity of computational results on the degree of basis set completeness for these processes is of note in future ab initio studies on Ru-catalyzed water oxidation. (2) Second, sizable Ru 4s4p core−valence correlation effects (>1 kcal/mol) were observed in some processes, like reactions 1, 3, and 6 and the end-on/side-on gap of the $[Ru^{IV}{-}OO]^{2+}$ intermediate. Concerning the direction of the Ru 4s4p core−valence correlation effect, we found that for reactions 2, 5, 6, and 8 and end-on/side-on gaps of $[Ru^{IV}{-}OO]^{2+}$ and $[Ru^{V}{-}OO]^{3+}$, its direction is the same as that of the BSIE correction. This result means that in principle, a fortuitous error cancellation of the valence BSIE and Ru 4s4p core−valence correlation effect by neglecting both of them is not possible in these calculations.

Having the coupled cluster reference data in hand now, we could start to assess the performances of various DFT methods on all those energetics included in Table 2. The tested functionals include PBE0,[66] M06,[67] M06-L,[67a] M06-2X,[67] TPSS,[68] TPSSh,[68] B3LYP,[69] CAM-B3LYP,[70] BP86,[71] B2GP-PLYP,[72] B2-PLYP,[73] OLYP,[69b,74] wB97X,[75] and BMK.[76] In Table 3, we summarized all the deviations of our DFT results from the coupled cluster reference data for 14 commonly used and popular approximate functionals in association with a very large QZ basis set. In contrast to the TZ basis set usually accurate enough in DFT calculations, here the necessity to go beyond it to reach the very large QZ basis set for DFT calculations can be seen from the fact that differences of some calculated energetics between the TZ and QZ level are still larger than 1 kcal/mol (see Table S1 in the SI for details). This result indicates that in some mononuclear Ru-based WOC processes, basis set convergence for DFT may not be as fast as usually considered in transition metal complexes, like the Au−alkene/alkyne/allene interaction and hydrogen abstraction barrier with high-valent $Fe^{IV}{=}O$ species, wherein a study showed that the TZ basis set has well converged the DFT calculations.[60,77] The LANL2DZ basis set of double-ζ quality,[78] which is often used in the computational study of transition metal systems, was also tested here for reaction 7. Compared to the QZ result, a deviation of about 12 kcal/mol was obtained (see Table S2 in the SI) with LANL2DZ, indicating that using the LANL2DZ basis set here for our WOC model system could also suffer from a severe basis set completeness problem. For O−O bond forming reaction 4 with all tested hybrid functionals, we observed that there is apparent spin contamination in its reactant and transition state (see Table S3 in the SI). Thus, we also performed Yamaguchi's spin projection procedure[79] for these two structures. Below, we separately analyze and discuss the DFT results of various reactions in Table 3.

First, in the whole catalytic cycle of water oxidation, WNA O−O bond formation was often suggested experimentally to be

dx.doi.org/10.1021/ct400004j | J. Chem. Theory Comput. 2013, 9, 1872−1879

the rate limiting step.[11,28,80] Concerning this most extensively studied process (eq 4) in theoretical modelings,[11,12,15,17,31,32,36−38] we surveyed both its reaction energy and barrier. For the reaction barrier, encouragingly our results show that some commonly used popular hybrid functionals perform very well, like PBE0, B3LYP, and M06, with deviations of −0.34, 0.69, and 1.90 kcal/mol, respectively. In addition to the O−O bond formation barrier height, the success of these functionals in the WNA process is also corroborated by the calculated reaction energy, which also prevents us from recommending other tested functionals. It is of note that these functionals are all hybrid ones, and no pure GGA or meta-GGA functional works well, especially for reaction energy. All tested pure (meta-)GGA functionals (BP86, M06-L, TPSS, OLYP) severely overestimate the reaction energy, i.e., destabilizing too much the O−O bond formed intermediate $Ru^{III}OOH$ relative to its reactant $Ru^{V}O$, while those hybrid functionals with a high percentage of Hartree−Fock (HF) exchange like BMK (42%) and M06-2X (54%) severely underestimate it. Thus, apparently more HF exchange tends to stabilize $Ru^{III}OOH$ relative to $Ru^{V}O$ and thus decrease its reaction energy. It appears that the medium HF exchanges in PBE0 (25%), B3LYP (20%), and M06 (27%) are just optimal here for describing the WNA process. This result also proves that previous choices of B3LYP, PBE0, and M06 for describing WNA O−O bond formation process are well-founded.[11,12,17,31,32,38] In contrast to our previous findings of good performance in closed-shell 4d and 5d transition metal systems including Rh, Pd, Pt, Ir, and Au,[60−62] double hybrid density functionals (DHDFTs) B2-PLYP and B2GP-PLYP herein are the two worst performing ones of all DFTs in the WNA barrier calculation of this open-shell system, albeit B2GP-PLYP produces a good reaction energy result. Concerning the spin contamination issue, spin projection generally decreases the stability of $Ru^{III}OOH$ relative to its $Ru^{V}O$ and increases the barrier correspondingly. Although beneficial for some functionals, we do not find that spin contamination correction for the WNA process can provide a uniform improvement for all hybrid functionals tested herein compared with the uncorrected values.

Second, for the O_2 release process, which was implied to be the rate limiting step in water oxidation by some mononuclear Ru-based WOCs,[10,18,29,30] we checked the reaction energy from both $Ru^{IV}O_2$ (eq 6) and $Ru^{V}O_2$ (eq 8) intermediates (note that both RuO_2 intermediates are in side-on conformation). The best performing functional of all is found to be TPSSh, with both absolute deviations of less than 2 kcal/mol. Similar to the reaction energy of WNA O−O bond formation, more HF exchange tends to decrease the O_2 release reaction energy, as seen clearly from TPSS/TPSSh and M06-L/M06/M06-2X results. Two DHDFTs give quite good reaction energy for $Ru^{IV}O_2$ but not for $Ru^{V}O_2$, presumably because the former is a closed-shell system while the latter is not. Thus, open-shell transition metal systems may still remain a great challenge for DHDFTs, as found before in iron-oxo systems.[77] Commonly used functionals B3LYP, PBE0, and M06 underestimate the O_2 release reaction energies evenly from both $Ru^{IV}O_2$ and $Ru^{V}O_2$ intermediates, by about 4−8 kcal/mol, with M06 having the smallest deviation among the three. Some pure (meta-)GGA functionals like M06L and OLYP give even better results than M06. However, their performance is not balanced between $Ru^{IV}O_2$ and $Ru^{V}O_2$, resulting in somewhat different deviations for these two species.

Third, the 1e-oxidation processes from $Ru^{IV}O$ (eq 3) and $Ru^{IV}O_2$ (eq 7) are directly related to their redox potential calculations.[12,15,30,38] Unfortunately, from Table 3 we found that there is no single functional that can simultaneously give good results for both cases. For $Ru^{IV}O$ oxidation energy, several pure (meta-)GGAs, like BP86, M06-L, TPSS, and two DHDFTs, perform well with deviations less than 2 kcal/mol. For the $Ru^{IV}O_2$ oxidation energy, only BMK and CAM-B3LYP give a deviation of less than 2 kcal/mol. Interestingly, deviations of $Ru^{IV}O_2$ oxidation energy generated from all functionals are about 10 kcal/mol smaller than the corresponding $Ru^{IV}O$ oxidation energy, with the exception of only two DHDFTs. This indicates that there is consistent bias of the DFTs (excluding DHDFTs) between $Ru^{IV}O$ and $Ru^{IV}O_2$ oxidation energies. In contrast to decreasing the reaction energies (eqs 4, 6, and 8) discussed above, for these two 1e-oxidation reactions 3 and 7, HF exchange tends to increase the reaction energy, i.e., destabilizing the Ru^{V} species compared to the corresponding Ru^{IV} reactants, as seen from TPSS/TPSSh and M06-L/M06/M06-2X results. However, if we notice that reactions 4, 6, and 8 discussed above are reductive type reactions with a lowering formal oxidation state of Ru, while reactions 3 and 7 are oxidative type reactions with an increasing formal oxidation state of Ru, we then come to a consistent trend that HF exchange increases the reaction energy of oxidative type reactions, and for reductive type reactions the opposite is true. We will see below that this trend about the reaction energy is general and also holds for other redox type reactions in the catalytic cycle.

Last, in the whole water oxidation catalytic cycle, the PCET processes to promote the oxidation state of Ru WOC in a cascade manner are essential steps before (eqs 1 and 2) and after (eq 5) O−O bond formation. These PCET processes constitute many PCET redox couples often encountered in Ru-based WOC. For PCET from $Ru^{II}OH_2$ (eq 1) and $Ru^{III}OH$ (eq 2), our calculations indicate that wB97X is the best functional, and B3LYP performs reasonably well. However, for PCET from $Ru^{III}OOH$ (eq 5), our calculations show that it is pure (meta-)GGAs (TPSS and OLYP) and DHDFTs, but not the two optimal hybrid functionals wB97X and B3LYP for PCET from $Ru^{II}OH_2$ and $Ru^{III}OH$, that perform well. Consistent with the trend outlined above on the effect of HF exchange in DFT, for these oxidative PCET processes, HF exchange tends to increase the reaction energies, as seen from TPSS/TPSSh and M06-L/M06/M06-2X data.

Except those key reactions in the water oxidation catalytic cycle, we also explored the interesting issue of $Ru−O_2$ side-on/end-on (closed/open) structure energetics. From the last two rows in Table 3, we know that to a different degree, all tested DFTs underestimate the stability of side-on $Ru^{IV}−O_2$ structure compared with the corresponding end-on one. The least underestimating DFTs are DHDFTs, with a minimum absolute deviation of about 4 kcal/mol from B2GP-PLYP. All the non-DHDFTs including B3LYP give substantial absolute deviation more than 10 kcal/mol. Such severe underestimation of the stability of the side-on $Ru^{IV}O_2$ structure by many commonly used DFTs would significantly affect our understanding of processes associated with $Ru^{IV}−O_2$ species and deserves special attention in future DFT calculations concerning this species. This finding is especially relevant to previous DFT energetic calculations reporting that the end-on triplet RuO_2 is more stable than the singlet side-on one,[9,30,38] which was found by Fujita et al. to be conflicting evidence against the assignment of $Ru^{IV}O_2$ species to a singlet side-on one.[9] Most likely, the stability of the singlet side-on $Ru^{IV}O_2$ structure was underestimated by DFT. Turning to $Ru^{V}−O_2$, although almost all tested DFTs except pure (meta-)GGAs still underestimate the stability of the $Ru^{V}−O_2$ side-on structure compared with the end-on one, now we have

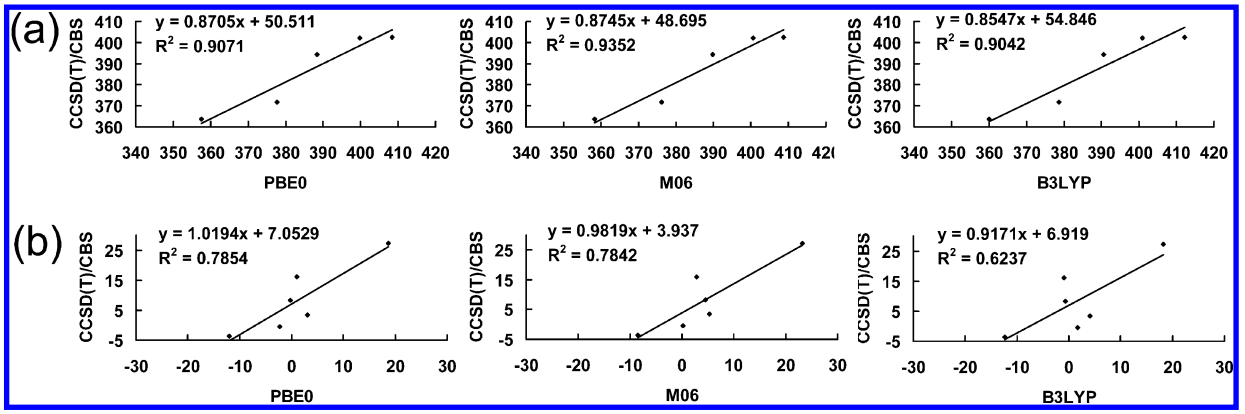

Figure 2. Correlation between reference CCSD(T) and DFT (PBE0, M06, and B3LYP) results for (a) five larger energetics ($\Delta E_R(1)$, $\Delta E_R(2)$, $\Delta E_R(3)$, $\Delta E_R(5)$, $\Delta E_R(7)$) and (b) the rest of the energetics.

several choices of functionals for good performance. These well performing functionals are M06-L, TPSSh, and OLYP, with an absolute deviation of about 1 kcal/mol.

To investigate the overall performance for the trend by DFT, we have done the correlation analysis between various DFT methods and the reference CCSD(T) method. For three functionals found above to be the best for the WNA step, i.e., PBE0, M06, and B3LYP, the correlation results are shown in Figure 2. Those results for the rest of the functionals are relegated to the SI (see Figures S1 and S2). Due to large difference in magnitudes of 11 investigated energetics as shown in Table 2, to distinguish between various functionals we did the correlation analysis for the five apparently larger energetics ($\Delta E_R(1)$, $\Delta E_R(2)$, $\Delta E_R(3)$, $\Delta E_R(5)$, $\Delta E_R(7)$) and for the rest separately. It can be seen that if an accurate description of energetics of the important WNA step is required, then PBE0 and M06 may be recommended in the whole catalytic cycle for trend calculations. However, B3LYP is only slightly inferior to them.

Finally, concerning the empirical dispersion correction for DFT, we tested Grimme's DFT-D3 method,[81−83] the detailed results of which are relegated to the SI (Tables S4 and S5 in). For almost all energy items (see Table S4), no apparent empirical dispersion correction was observed except reaction 8, which has a mean absolute correction of about 1.3 kcal/mol over all DFT methods. While for all the other reactions, relatively large empirical dispersion corrections were only seen with wB97X/OLYP, which has a mean absolute correction of 1.80/1.67 kcal/mol over all energy items in Table 2. For B2GP-PLYP and PBE0, all DFT-D3 results have a certain degree of improvement, while for other functionals, DFT-D3 corrections do not uniformly improve the results. In general, the magnitudes of DFT-D3 corrections are small compared with deviations of corresponding DFT results from the CCSD(T) reference data, and no sign of deviation is changed by inclusion of the DFT-D3 corrections (see Table S5). This generally small dispersion correction could be due to the less bulky character of the ammonia ligand in our model system, and other more bulky ligands in WOCs may bring larger effect.

In this work, using a high level ab initio CCSD(T) protocol as reference tool, we report the first systematic assessment on the performance of various DFTs in the whole catalytic cycle of water oxidation by a simplified model system of a single site Ru-based WOC. Our main findings are summarized as follows: (1) For the WNA O−O bond formation reaction, commonly used B3LYP, PBE0, and M06 functionals can produce a quite accurate reaction energy and barrier. (2) For the O_2 release reaction energy from both Ru^{IV}−O_2 and Ru^{V}−O_2 species, TPSSh is the best performing functional among all 14 DFTs tested. (3) For the 1e-oxidation reaction energies of Ru^{IV}−O and Ru^{IV}−O_2, there is a systematic bias of around 10 kcal/mol using DFT methods (except DHDFT) between them. For the $Ru^{IV}O$ oxidation energy, pure (meta-)GGAs BP86, M06-L, TPSS, and two DHDFTs perform well, while for the $Ru^{IV}O_2$ oxidation energy, only BMK and CAM-B3LYP give good results. (4) For the PCET oxidation reactions from $Ru^{II}OH_2$ and $Ru^{III}OH$, hybrid functional wB97X and B3LYP are the best, while for the PCET oxidation reaction from $Ru^{III}OOH$, pure (meta-)GGAs TPSS and OLYP and DHDFT B2-PLYP are the best ones. (5) Concerning the Ru−O_2 side-on/end-on relative energetics issue, our results indicate that all 14 tested DFTs underestimate the stability of the Ru^{IV}−O_2 side-on structure compared with the end-on structure by mostly more than 10 kcal/mol. Whereas Ru^{V}−O_2 stability remains largely underestimated by most DFTs, M06-L, TPSSh, and OLYP can produce a quite accurate energy gap between side-on and end-on Ru^{V}−O_2 species. (6) Generally, HF exchange in DFT is found to increase the oxidative reaction energy and oppositely to decrease the reductive reaction energy. From the above findings, it is clear that using single approximate DFT to accurately model all reactions involved in the WOC catalytic cycle is still very difficult and challenging currently. Despite this unsatisfactory aspect, considering the descriptions of both WNA step energetics and the trend of the whole catalytic cycle, PBE0 and M06 may be recommended for Ru-based WOCs in the current status.

Finally, from the experience gained in this work, we want to notify the community that for ab initio CCSD(T) methods as well as DFT methods, it is likely that the basis set incompleteness effect is unusually quite severe in some reactions and processes of Ru-based WOCs, especially those involving $Ru^{IV/V}$−O_2 species. This unexpected basis set sensitivity would necessitate employing a larger basis set, at least for testing purposes, to avoid affecting qualitative aspects of the computational results.

■ ASSOCIATED CONTENT

Ⓢ Supporting Information

Computational details, seven tables and two figures of computational results, and Cartesian coordinates of all species. This material is available free of charge via the Internet at http://pubs.acs.org.

■ AUTHOR INFORMATION

Corresponding Author

*E-mail: jnyao@iccas.ac.cn (J.Y.). chenh@iccas.ac.cn (H.C.).

Notes

The authors declare no competing financial interest.

■ ACKNOWLEDGMENTS

This work was supported by the Chinese Academy of Sciences, NSFC (No. 21290194), and National Basic Research Program of China (No. 2011CB808402). The authors thank Dr. J. Grant Hill for providing the Ru cc-pwCVTZ-PP/MP2FIT auxiliary basis set before its publication, which was used in this work for the explicitly correlated coupled cluster calculations of 4s4p core−valence correlation effect.

■ REFERENCES

(1) (a) Lewis, N. S.; Nocera, D. G. *Proc. Natl. Acad. Sci. U. S. A.* **2006**, *103*, 15729−15735. (b) Cook, T. R.; Dogutan, D. K.; Reece, S. Y.; Surendranath, Y.; Teets, T. S.; Nocera, D. G. *Chem. Rev.* **2010**, *110*, 6474−6502. (c) Balzani, V.; Credi, A.; Venturi, M. *ChemSusChem* **2008**, *1*, 26−58. (d) Armaroli, N.; Balzani, V. *Angew. Chem., Int. Ed.* **2007**, *46*, 52−66. (e) Gust, D.; Moore, T. A.; Moore, A. L. *Acc. Chem. Res.* **2009**, *42*, 1890−1898.

(2) Umena, Y.; Kawakami, K.; Shen, J.-R.; Kamiya, N. *Nature* **2011**, *473*, 55−60.

(3) (a) McEvoy, J. P.; Brudvig, G. W. *Chem. Rev.* **2006**, *106*, 4455−4483. (b) Lubitz, W.; Reijerse, E. J.; Messinger, J. *Energy Environ. Sci.* **2008**, *1*, 15−31.

(4) (a) Sun, L. C.; Hammarström, L.; Åkermark, B.; Styring, S. *Chem. Soc. Rev.* **2001**, *30*, 36−49. (b) Lv, H. J.; Geletii, Y. V.; Zhao, C. C.; Vickers, J. W.; Zhu, G. B.; Luo, Z.; Song, J.; Lian, T. Q.; Musaev, D. G.; Hill, C. L. *Chem. Soc. Rev.* **2012**, *41*, 7572−7589.

(5) (a) Rüttinger, W.; Dismukes, G. C. *Chem. Rev.* **1997**, *97*, 1−24. (b) Yagi, M.; Kaneko, M. *Chem. Rev.* **2001**, *101*, 21−35.

(6) (a) Concepcion, J. J.; Jurss, J. W.; Brennaman, M. K.; Hoertz, P. G.; Patrocinio, A. O. T.; Iha, N. Y. M.; Templeton, J. L.; Meyer, T. J. *Acc. Chem. Res.* **2009**, *42*, 1954−1965. (b) Gagliardi, C. J.; Vannucci, A. K.; Concepcion, J. J.; Chen, Z.; Meyer, T. J. *Energy Environ. Sci.* **2012**, *5*, 7704−7717.

(7) (a) Yamazaki, H.; Shouji, A.; Kajita, M.; Yagi, M. *Coord. Chem. Rev.* **2010**, *254*, 2483−2491. (b) Dau, H.; Limberg, C.; Reier, T.; Risch, M.; Roggan, S.; Strasser, P. *ChemCatChem* **2010**, *2*, 724−761. (c) Liu, X.; Wang, F. *Coord. Chem. Rev.* **2012**, *256*, 1115−1136. (d) Limburg, B.; Bouwman, E.; Bonnet, S. *Coord. Chem. Rev.* **2012**, *256*, 1451−1467.

(8) (a) Cao, R.; Lai, W. Z.; Du, P. W. *Energy Environ. Sci.* **2012**, *5*, 8134−8157. (b) Hetterscheid, D. G. H.; Reek, J. N. H. *Angew. Chem., Int. Ed.* **2012**, *51*, 9740−9747. (c) Wasylenko, D. J.; Palmer, R. D.; Berlinguette, C. P. *Chem. Commun.* **2013**, *49*, 218−227.

(9) Polyansky, D. E.; Muckerman, J. T.; Rochford, J.; Zong, R. F.; Thummel, R. P.; Fujita, E. *J. Am. Chem. Soc.* **2011**, *133*, 14649−14665.

(10) Concepcion, J. J.; Tsai, M. K.; Muckerman, J. T.; Meyer, T. J. *J. Am. Chem. Soc.* **2010**, *132*, 1545−1557.

(11) Chen, Z. F.; Concepcion, J. J.; Hu, X. Q.; Yang, W. T.; Hoertz, P. G.; Meyer, T. J. *Proc. Natl. Acad. Sci. U. S. A.* **2010**, *107*, 7225−7229.

(12) Wang, L.-P.; Wu, Q.; Voorhis, T. V. *Inorg. Chem.* **2010**, *49*, 4543−4553.

(13) Tong, L. P.; Wang, Y.; Duan, L. L.; Xu, Y. H.; Cheng, X.; Fischer, A.; Ahlquist, M. S. G.; Sun, L. C. *Inorg. Chem.* **2012**, *51*, 3388−3398.

(14) Duan, L. L.; Bozoglian, F.; Mandal, S.; Stewart, B.; Privalov, T.; Llobet, A.; Sun, L. C. *Nat. Chem* **2012**, *4*, 418−423.

(15) Vigara, L.; Ertem, M. Z.; Planas, N.; Bozoglian, F.; Leidel, N.; Dau, H.; Haumann, M.; Gagliardi, L.; Cramer, C. J.; Llobet, A. *Chem. Sci* **2012**, *3*, 2576−2586.

(16) Kimoto, A.; Yamauchi, K.; Yoshida, M.; Masaoka, S.; Sakai, K. *Chem. Commun.* **2012**, *48*, 239−241.

(17) Tong, L. P.; Duan, L. L.; Xu, Y. H.; Privalov, T.; Sun, L. C. *Angew. Chem., Int. Ed.* **2011**, *50*, 445−449.

(18) Concepcion, J. J.; Jurss, J. W.; Templeton, J. L.; Meyer, T. J. *J. Am. Chem. Soc.* **2008**, *130*, 16462−16463.

(19) Yamazaki, H.; Hakamata, T.; Komi, M.; Yagi, M. *J. Am. Chem. Soc.* **2011**, *133*, 8846−8849.

(20) Boyer, J. L.; Polyansky, D. E.; Szalda, D. J.; Zong, R. F.; Thummel, R. P.; Fujita, E. *Angew. Chem., Int. Ed.* **2011**, *50*, 12600−12604.

(21) Wang, L.; Duan, L. L.; Stewart, B.; Pu, M. P.; Liu, J. H.; Privalov, T.; Sun, L. C. *J. Am. Chem. Soc.* **2012**, *134*, 18868−18880.

(22) Kohl, S. W.; Weiner, L.; Schwartsburd, L.; Konstantinovski, L.; Shimon, L. J. W.; Ben-David, Y.; Iron, M. A.; Milstein, D. *Science* **2009**, *324*, 74−77.

(23) Yoshida, M.; Masaoka, S.; Abe, J.; Sakai, K. *Chem. Asian J.* **2010**, *5*, 2369−2378.

(24) Tseng, H.-W.; Zong, R. F.; Muckerman, J. T.; Thummel, R. P. *Inorg. Chem.* **2012**, *47*, 11763−11773.

(25) Tsai, M.-K.; Rochford, J.; Polyansky, D. E.; Wada, T.; Tanaka, K.; Fujita, E.; Muckerman, J. T. *Inorg. Chem.* **2009**, *48*, 4372−4383.

(26) Wasylenko, D. J.; Ganesamoorthy, C.; Koivisto, B. D.; Henderson, M. A.; Berlinguette, C. P. *Inorg. Chem.* **2010**, *49*, 2202−2209.

(27) Radaram, B.; Ivie, J. A.; Singh, W. M.; Grudzien, R. M.; Reibenspies, J. H.; Webster, C. E.; Zhao, X. *Inorg. Chem.* **2011**, *50*, 10564−10571.

(28) Murakami, M.; Hong, D. C.; Suenobu, T.; Yamaguchi, S.; Ogura, T.; Fukuzumi, S. *J. Am. Chem. Soc.* **2011**, *133*, 11605−11613.

(29) Wasylenko, D. J.; Ganesamoorthy, C.; Henderson, M. A.; Koivisto, B. D.; Osthoff, H. D.; Berlinguette, C. P. *J. Am. Chem. Soc.* **2010**, *132*, 16094−16106.

(30) Lin, X. S.; Hu, X. Q.; Concepcion, J. J.; Chen, Z. F.; Liu, S. B.; Meyer, T. J.; Yang, W. T. *Proc. Natl. Acad. Sci. U. S. A.* **2012**, *109*, 15669−15672.

(31) Lai, W. Z.; Cao, R.; Dong, G.; Shaik, S.; Yao, J. N.; Chen, H. *J. Phys. Chem. Lett.* **2012**, *3*, 2315−2319.

(32) Privalov, T.; Kermark, B.; Sun, L. C. *Chem.—Eur. J.* **2011**, *17*, 8313−8317.

(33) Chen, Y.; Fang, W. H. *J. Phys. Chem. A* **2010**, *114*, 10334−10338.

(34) Yang, X. Z.; Hall, M. B. *J. Am. Chem. Soc.* **2010**, *132*, 120−130.

(35) Nyhlén, J.; Duan, L. L.; Åkermark, B.; Sun, L. C.; Privalov, T. *Angew. Chem., Int. Ed.* **2010**, *49*, 1773−1777.

(36) Vallés-Pardo, J. L.; Guijt, M. C.; Iannuzzi, M.; Joya, K. S.; de Groot, H. J. M.; Buda, F. *ChemPhysChem* **2012**, *13*, 140−146.

(37) Sala, X.; Ertem, M. Z.; Vigara, L.; Todorova, T. K.; Chen, W. Z.; Rocha, R. C.; Aquilante, F.; Cramer, C. J.; Gagliardi, L.; Llobet, A. *Angew. Chem., Int. Ed.* **2010**, *49*, 7745−7747.

(38) Hughes, T. F.; Friesner, R. A. *J. Phys. Chem. B* **2011**, *115*, 9280−9289.

(39) Niu, S. Q.; Hall, M. B. *Chem. Rev.* **2000**, *100*, 353−405.

(40) Siegbahn, P. E. M.; Blomberg, M. R. A. *Chem. Rev.* **2000**, *100*, 421−437.

(41) Torrent, M.; Solà, M.; Frenking, G. *Chem. Rev.* **2000**, *100*, 439−493.

(42) Noodleman, L.; Lovell, T.; Han, W.-G.; Li, J.; Himo, F. *Chem. Rev.* **2004**, *104*, 459−508.

(43) Cramer, C. J.; Truhlar, D. G. *Phys. Chem. Chem. Phys.* **2009**, *11*, 10757−10816.

(44) Balcells, D.; Clot, E.; Eisenstein, O. *Chem. Rev.* **2010**, *110*, 749−823.

(45) Shaik, S.; Cohen, S.; Wang, Y.; Chen, H.; Kumar, D.; Thiel, W. *Chem. Rev.* **2010**, *110*, 949−1017.

(46) Chen, H.; Lai, W. Z.; Shaik, S. *J. Phys. Chem. B* **2011**, *115*, 1727−1742.

(47) Harvey, J. N. *J. Biol. Inorg. Chem.* **2011**, *16*, 831−839.

(48) Knowles, P. J.; Hampel, C.; Werner, H.-J. *J. Chem. Phys.* **1993**, *99*, 5219−5227.

(49) Watts, J. D.; Gauss, J.; Bartlett, R. J. *J. Chem. Phys.* **1993**, *98*, 8718−8733.

(50) Knizia, G.; Adler, T. B.; Werner, H.-J. *J. Chem. Phys.* **2009**, *130*, 054104.

(51) Romain, S.; Vigara, L.; Llobet, A. *Acc. Chem. Res.* **2009**, *42*, 1944−1953.
(52) Meyer, T. J.; Huynh, M. H. V.; Thorp, H. H. *Angew. Chem., Int. Ed.* **2007**, *46*, 5284−5304.
(53) Bell, R. P. *Proc. R. Soc. London, Ser. A* **1936**, *154*, 414−421.
(54) Evans, M. G.; Polanyi, M. *Trans. Faraday Soc.* **1938**, *34*, 11−24.
(55) Peterson, K. A.; Figgen, D.; Dolg, M.; Stoll, H. *J. Chem. Phys.* **2007**, *126*, 124101.
(56) Dunning, T. H., Jr. *J. Chem. Phys.* **1989**, *90*, 1007−1023.
(57) Lee, T. J.; Taylor, P. R. *Int. J. Quantum Chem.* **1989**, *23*, 199−207.
(58) Frisch, M. J.; Trucks, G. W.; Schlegel, H. B.; Scuseria, G. E.; Robb, M. A.; Cheeseman, J. R.; Scalmani, G.; Barone, V.; Mennucci, B.; Petersson, G. A.; Nakatsuji, H.; Caricato, M.; Li, X.; Hratchian, H. P.; Izmaylov, A. F.; Bloino, J.; Zheng, G.; Sonnenberg, J. L.; Hada, M.; Ehara, M.; Toyota, K.; Fukuda, R.; Hasegawa, J.; Ishida, M.; Nakajima, T.; Honda, Y.; Kitao, O.; Nakai, H.; Vreven, T.; Montgomery, J. A., Jr.; Peralta, J. E.; Ogliaro, F.; Bearpark, M.; Heyd, J. J.; Brothers, E.; Kudin, K. N.; Staroverov, V. N.; Kobayashi, R.; Normand, J.; Raghavachari, K.; Rendell, A.; Burant, J. C.; Iyengar, S. S; Tomasi, J.; Cossi, M.; Rega, N.; Millam, J. M.; Klene, M.; Knox, J. E.; Cross, J. B.; Bakken, V.; Adamo, C.; Jaramillo, J.; Gomperts, R.; Stratmann, R. E.; Yazyev, O.; Austin, A. J.; Cammi, R.; Pomelli, C.; Ochterski, J. W.; Martin, R. L.; Morokuma, K.; Zakrzewski, V. G.; Voth, G. A.; Salvador, P.; Dannenberg, J. J.; Dapprich, S.; Daniels, A. D.; Farkas, O.; Foresman, J. B.; Ortiz, J. V.; Cioslowski, J.; Fox, D. J. *Gaussian 09*, revision C.01; Gaussian, Inc.: Wallingford, CT, 2009.
(59) Werner, H.-J.; Knowles, P. J.; Lindh, R.; Manby, F. R.; Schütz, M.; Celani, P.; Korona, T.; Mitrushenkov, A.; Rauhut, G.; Adler, T. B.; Amos, R. D.; Bernhardsson, A.; Berning, A.; Cooper, D. L.; Deegan, M. J. O.; Dobbyn, A. J.; Eckert, F.; Goll, E.; Hampel, C.; Hetzer, G.; Hrenar, T.; Knizia, G.; Köppl, C.; Liu, Y.; Lloyd, A. W.; Mata, R. A.; May, A. J.; McNicholas, S. J.; Meyer, W.; Mura, M. E.; Nicklass, A.; Palmieri, P.; Pflüger, K.; Pitzer, R.; Reiher, M.; Schumann, U.; Stoll, H.; Stone, A. J.; Tarroni, R.; Thorsteinsson, T.; Wang, M.; Wolf, A. MOLPRO, version 2010.1, a package of ab initio programs. See http://www.molpro.net.
(60) Kang, R. H.; Chen, H.; Shaik, S.; Yao, J. N. *J. Chem. Theory Comput.* **2011**, *7*, 4002−4011.
(61) Kang, R. H.; Lai, W. Z.; Yao, J. N.; Shaik, S.; Chen, H. *J. Chem. Theory Comput.* **2012**, *8*, 3119−3127.
(62) Lai, W. Z.; Yao, J. N.; Shaik, S.; Chen, H. *J. Chem. Theory Comput.* **2012**, *8*, 2991−2996.
(63) Chen, K. J.; Zhang, G. L.; Chen, H.; Yao, J. N.; Danovich, D.; Shaik, S. *J. Chem. Theory Comput.* **2012**, *8*, 1641−1645.
(64) Chen, H.; Lai, W. Z.; Yao, J. N.; Shaik, S. *J. Chem. Theory Comput.* **2011**, *7*, 3049−3053.
(65) Chen, H.; Cho, K.-B.; Lai, W. Z.; Nam, W.; Shaik, S. *J. Chem. Theory Comput.* **2012**, *8*, 915−926.
(66) (a) Perdew, J. P.; Burke, K.; Ernzerhof, M. *Phys. Rev. Lett.* **1996**, *77*, 3865−3868. (b) Ernzerhof, M.; Scuseria, G. E. *J. Chem. Phys.* **1999**, *110*, 5029−5036. (c) Adamo, C.; Barone, V. *J. Chem. Phys.* **1999**, *110*, 6158−6170.
(67) (a) Zhao, Y.; Truhlar, D. G. *J. Chem. Phys.* **2006**, *125*, 194101. (b) Zhao, Y.; Truhlar, D. G. *Theor. Chem. Acc.* **2008**, *120*, 215−241.
(68) Tao, J.; Perdew, J. P.; Staroverov, V. N.; Scuseria, G. E. *Phys. Rev. Lett.* **2003**, *91*, 146401.
(69) (a) Becke, A. D. *Phys. Rev. A* **1988**, *38*, 3098−3100. (b) Lee, C.; Yang, W.; Parr, R. G. *Phys. Rev. B* **1988**, *37*, 785−789. (c) Becke, A. D. *J. Chem. Phys.* **1993**, *98*, 5648−5652.
(70) Yanai, T.; Tew, D.; Handy, N. *Chem. Phys. Lett.* **2004**, *393*, 51−57.
(71) (a) Becke, A. D. *Phys. Rev. A* **1988**, *38*, 3098−3100. (b) Perdew, J. P. *Phys. Rev. B* **1986**, *33*, 8822−8824.
(72) Karton, A.; Tarnopolsky, A.; Lamère, J.-F.; Schatz, G. C.; Martin, J. M. L. *J. Phys. Chem. A* **2008**, *112*, 12868−12886.
(73) Grimme, S. *J. Chem. Phys.* **2006**, *124*, 034108.
(74) Handy, N. C.; Cohen, A. J. *Mol. Phys.* **2001**, *99*, 403−412.
(75) Chai, J.-D.; Head-Gordon, M. *J. Chem. Phys.* **2008**, *128*, 084106.
(76) Boese, A. D.; Martin, J. M. L. *J. Chem. Phys.* **2004**, *121*, 3405−3416.
(77) Chen, H.; Lai, W. Z.; Shaik, S. *J. Phys. Chem. Lett.* **2010**, *1*, 1533−1540.
(78) Hay, P. J.; Wadt, W. R. *J. Chem. Phys.* **1985**, *82*, 299−310.
(79) Yamaguchi, K.; Jensen, F.; Dorigo, A.; Houk, K. N. *Chem. Phys. Lett.* **1988**, *149*, 537−542.
(80) Wasylenko, D. J.; Ganesamoorthy, C.; Henderson, M. A.; Berlinguette, C. P. *Inorg. Chem.* **2011**, *50*, 3662−3672.
(81) Grimme, S.; Antony, J.; Ehrlich, S.; Krieg, H. *J. Chem. Phys.* **2010**, *132*, 154104.
(82) Goerigk, L.; Grimme, S. *J. Chem. Theory Comput.* **2011**, *7*, 291−309.
(83) (a)There are no DFT-D3 parameters for wB97X functional, thus empirical dispersion corrected functional wB97XD in ref 83b designed by the developers of wB97X was tested instead. (b) Chai, J.-D.; Head-Gordon, M. *Phys. Chem. Chem. Phys.* **2008**, *10*, 6615−6620.